Supplemental Information materials – Polyvinyl fluoride: Predicting polarization in a complex soft matter system

Carl M. Frostenson,[1] Pär A. T. Olsson,[2,3] and Per Hyldgaard[1]

[1] *Department of Microtechnology and Nanoscience-MC2, Chalmers University of Technology, SE-412 96 Göteborg, Sweden*
[2] *Materials Science and Applied Mathematics, Malmö University, SE-205 06 Malmö, Sweden*
[3] *Division of Mechanics, Materials & Component Design, Lund University, Box 118, SE-221 00 Lund, Sweden*

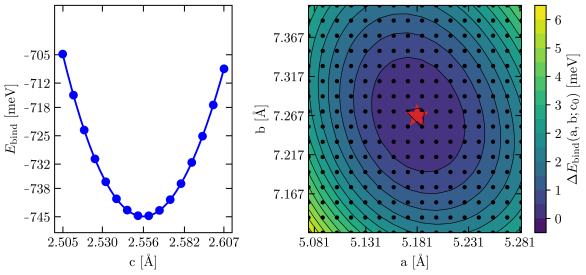

FIG. S1. Binding-energy mapping of GS-PVF.

Figure S1 summarizes a validation of our full-stress motif characterization for the GS PVF motif. We consider the stress-based unit-cell result (a_0', b_0', c_0') (identified by a red star), as validated since it exactly matches the minimum of the energy landscape in Fig. S1. Likewise Fig. S2 shows the detailed mapping of the binding-energy variation for ES1 (top row) and ES2 (bottom row). Again the results of the stress-based unit-cell optimizations are found to concur with those of the mapping approach. These results demonstrate consistency between the two approaches.

I. PVF STRUCTURE SEARCH

Table S I shows the results of the motif search via CX relaxations. It provides a summary of connections between original guesses 'Origin' and motifs/states. To accomplish that it lists and delineates unique characteristics of motifs. The discriminators include the structure itself, the predicted polarity, unit cell volume, and crystal binding energy (E_{bind}). To distinguish between the structures, two structures are deemed equivalent if: (a) the volume differences ΔV are less than 0.1 Å^3, (b) they possess identical polarity, (c) the energy variations in their relaxed states ΔE_{bind} are below 0.5 meV, and finally (d) they can be made congruent through a combination of rotations.

II. STRUCTURE-SEARCH VALIDATION

To validate the structure-search predictions (for GS and the first two ES) we use a 'map' technique. For the set of key PVF motifs (GS, ES1, and ES2,) we first consider a sequence of assumed c values for the unit-cell extension and for each of these we use constrained-variable-cell optimization (relaxing unit-cell constants a and b as well as atoms). Second, we identify the optimal c_0, as a minimum of paper Eq. (2), repeat the constrained-relaxation at that c_0 value, and extract the predictions for optimal-cell geometry (a_0, b_0, c_0) and binding-energy value $E_{\text{bind}}(a_0, b_0, c_0)$ for that motif. Third, we provide with a complete binding-energy mapping at the optimal c_0 value but at general a and b values.

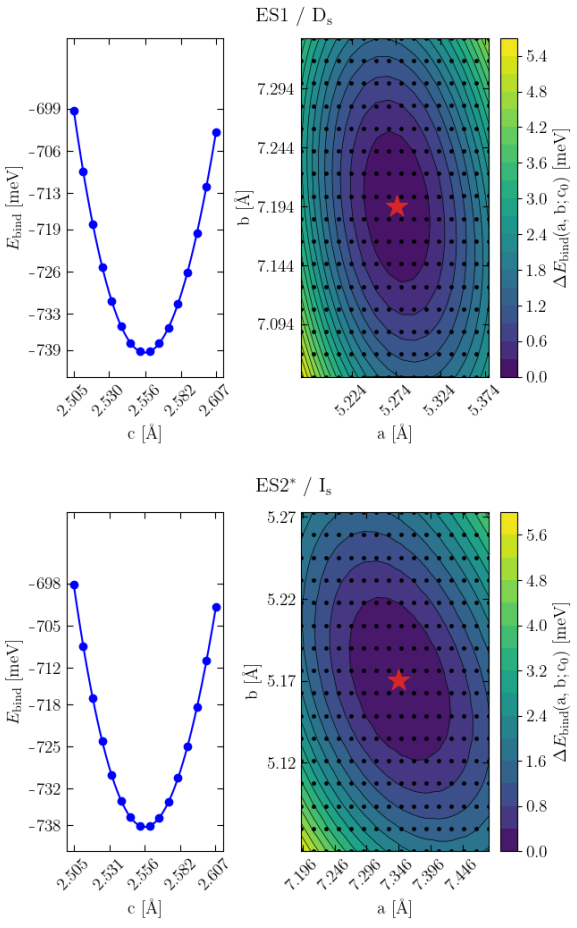

FIG. S2. Cohesive-energy mapping of the two the most relevant excited states of PVF: ES1 (top panels) and ES2 (bottom panels).

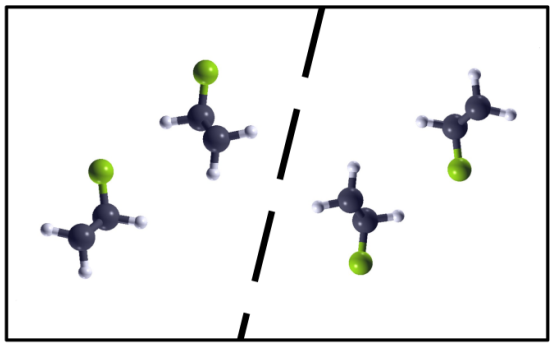

FIG. S3. Schematics of a crystalline PVF system formed entirely by the ES2 conformer but containing two domains of opposite polarization: Downwards (upwards) on the left (right) side of an assumed boundary (dashed line).

III. PVDF AND PVF ENERGY SCALES FOR POLARIZATION REVERSAL

The application an external electric field can adjust and, at least partly, reverse the polarization in the β-PVDF system, since it is possible to make poled samples. Given the similarity of the structure of the PVF ES2 motif and the β-PVDF system, it is relevant to discuss if the same is possible for PVF.

Figure S3 shows schematics of a crystalline PVF systems that is formed entirely by the ES2 conformer but containing a polarization boundary: For the ES2 domain on the left-hand side the polarization is pointing downward while the reverse holds for the right-hand-side domain. The application of, for example, an upwards pointing electrical field will then make the configuration in the right-side domain more energetically favorable. This energy difference could, in turn, produce a macroscopic polarization response, assuming the barriers for flipping the polarization is low enough that the external-field control remains practical.

Figure S4 illustrates and summarizes the set of twist-excitation calculations that we report to contrast the energy scales involved in an external-field flipping the spontaneous polarization in β-PVDF and in a would-be polar PVF system. Our study consider the GS geometries and computes the energy (upon constrained relaxations inside a super-cell setup) associated by twisting one chain while keeping a second chain fixed in the original geometry.

Figure S5 compares the computed energy costs of making such selective rotation. The twist process is one type of structural excitation that contributes to starting the β-PVDF polarization adjustment and reversal and in a polar PVF. For a crude discussion, we take the ratio of computed maxima (about 0.8 eV versus 0.5 eV, Fig. S5) of this β-PVDF and PVF energy variations as reflective of differences in the energy scale for electric-field induced reversal. We conclude that poling (operating a polar PVF system as a reversible ferroelectrics) likely present the same level of challenges in polar PVF and in β-PVDF.

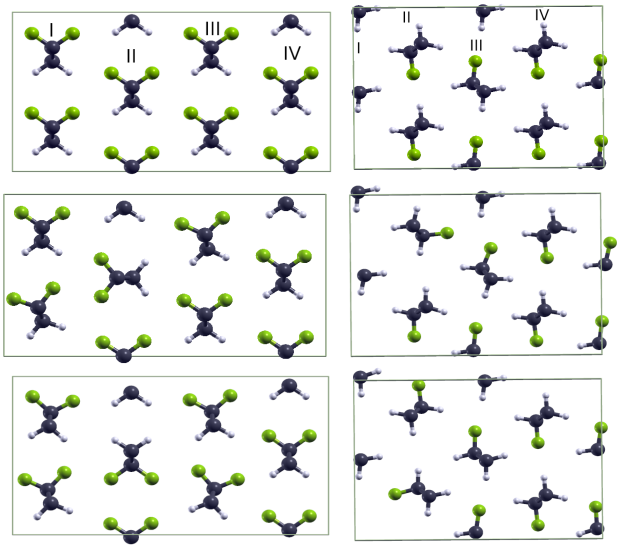

FIG. S4. Twist excitation in GS PVDF (left column of panels) and GS PVF (right column of panels). We consider $2 \times 2 \times 1$ super-cells of initially unperturbed GS geometries (top row of panels), numbering the columns of chains by roman numerals ('I' through 'IV') and always keeping the bottom chain at position 'IV' frozen as in the original GS configuration; The chains at maximum separation from this reference point is then the middle (top) chain at position 'II' for PVDF (for PVF). The middle (bottom) column of panels shows geometries that emerges (upon full relaxations of all other chains) as we rotate and freeze the position-'II' chain at 90° (180°).

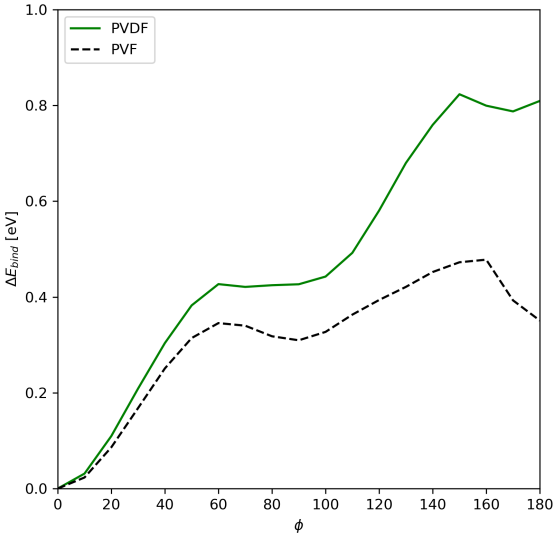

FIG. S5. Comparison of energy scale for twist excitations in GS PVDF (solid, green) and GS PVF (dashed, black). The computation procedure is described in Fig. S4.

TABLE S I. Table summarizing the physical properties of the investigated structural motifs of PVF. Each entry corresponds to a distinct structure characterized by its structure, polarity, unit cell volume and binding energy E_{bind}. Structures are differentiated by considering two states equivalent if (a) $\Delta\,\text{V} < 0.1$ Å^3, (b) relaxed structures have a minute energy difference, $\Delta E < 0.5$ meV, (c) the predicted spontaneous polarization agrees (a test used for GS, ES1, ES2), and finally (d) there exists some unit-cell transformation connecting structures.

ID	Origin	Structure	Polar	Volume [Å^3]	E_{bind} [meV]	Motif	State	ΔE_{bind} [meV]
19	G	Orth	No	96.095	-745.943	G_p	GS	-0.000
11	W	Orth	No	96.188	-745.537			0.406
5	E	Orth	Weakly	96.942	-740.456	D_s	ES1	5.487
4	D	Orth	Weakly	96.817	-740.397			5.545
24	L	Orth	Weakly	96.831	-740.107			5.836
9	I	Orth	Yes	96.997	-739.362	I_s	ES2	6.581
20	T	Orth	Yes	97.048	-739.073	T_s		6.870
3	C	Mono	No	96.194	-739.196	C_s	ES3	6.747
22	V	Mono	Yes	97.008	-738.455	V_a	ES4	7.487
16	P	Mono	Yes	96.650	-736.653	P_s	ES5	9.290
15	O	Orth	Yes	96.001	-736.272	O_s	ES6	9.671
23	K	Mono	Yes	97.182	-735.995	K_a	ES7	9.948
10	J	Mono	Yes	97.213	-735.980	J_s	ES8	9.963
17	Q	Mono	Yes	97.304	-735.888	H_s	ES9	10.055
8	H	Mono	Yes	97.210	-735.645			10.298
1	M	Mono	Yes	97.368	-735.273	M_a	ES10	10.670
14	B	Orth	Yes	97.608	-728.732	B_a	ES11	17.211
7	S	Mono	Yes	97.980	-724.382	S_a	ES12	21.561
2	N	Orth	Yes	98.018	-723.114	N_a	ES13	22.829
13	A	Mono	Yes	97.880	-721.484	A_a	ES14	24.459
21	U	Tri/Mono	Yes	98.439	-704.760	F_a	ES15	41.183
6	R	Tri/Mono	Yes	98.461	-704.701			41.242
12	X	Tri/Mono	Yes	98.623	-704.659			41.284
18	F	Tri/Mono	Yes	98.464	-704.573			41.369